Ancient Mycobacterium leprae genome reveals medieval English red squirrels as animal leprosy host

Urban, Christian ; Blom, Alette A ; Avanzi, Charlotte ; Walker-Meikle, Kathleen ; Warren, Alaine K ; White-Iribhogbe, Katie ; Turle, Ross ; Marter, Phil ; Dawson-Hobbis, Heidi ; Roffey, Simon ; Inskip, Sarah A ; Schuenemann, Verena J

DOI: https://doi.org/10.1016/j.cub.2024.04.006

Originally published at:
Urban, Christian; Blom, Alette A; Avanzi, Charlotte; Walker-Meikle, Kathleen; Warren, Alaine K; White-Iribhogbe, Katie; Turle, Ross; Marter, Phil; Dawson-Hobbis, Heidi; Roffey, Simon; Inskip, Sarah A; Schuenemann, Verena J (2024). Ancient Mycobacterium leprae genome reveals medieval English red squirrels as animal leprosy host. Current Biology, 34(10):2221-2230.e8.
DOI: https://doi.org/10.1016/j.cub.2024.04.006

Current Biology

CellPress
OPEN ACCESS

Report

Ancient *Mycobacterium leprae* genome reveals medieval English red squirrels as animal leprosy host

Christian Urban,[1,2,3,13] Alette A. Blom,[2,4,5,13] Charlotte Avanzi,[6,13] Kathleen Walker-Meikle,[1,2,7] Alaine K. Warren,[6] Katie White-Iribhogbe,[8] Ross Turle,[9] Phil Marter,[10] Heidi Dawson-Hobbis,[10] Simon Roffey,[10] Sarah A. Inskip,[5,*] and Verena J. Schuenemann[1,2,11,12,14,*]

[1]Institute of Evolutionary Medicine, University of Zurich, Winterthurerstrasse 190, 8057 Zurich, Switzerland
[2]Department of Environmental Sciences, University of Basel, Spalenring 145, 4055 Basel, Switzerland
[3]Functional Genomics Center Zurich, ETH Zurich and University of Zurich, Winterthurerstrasse 190, 8057 Zurich, Switzerland
[4]Department of Archaeology, University of Cambridge, Downing Street, Cambridge CB2 3ER, UK
[5]School of Archaeology and Ancient History, University of Leicester, University Road, Leicester LE1 7RH, UK
[6]Department of Microbiology, Immunology and Pathology, Colorado State University, 401 W Pitkin St, Fort Collins, CO 80523, USA
[7]Science Museum Group, Science Museum, Exhibition Road, South Kensington, London SW7 2DD, UK
[8]School of Oriental and African Studies (SOAS), University of London, 10 Thornaugh Street, London WC1H 0XG, UK
[9]Hampshire Cultural Trust, Chilcomb House, Chilcomb Lane, Winchester SO23 8RB, UK
[10]School of History, Archaeology and Philosophy, University of Winchester, Medecroft Building, Sparkford Road, Winchester SO22 4NH, UK
[11]Department of Evolutionary Anthropology, University of Vienna, Djerassiplatz 1, 1030 Vienna, Austria
[12]Human Evolution and Archaeological Sciences, University of Vienna, Djerassiplatz 1, 1030 Vienna, Austria
[13]These authors contributed equally
[14]Lead contact
*Correspondence: s.inskip@le.ac.uk (S.A.I.), verena.schuenemann@iem.uzh.ch (V.J.S.)
https://doi.org/10.1016/j.cub.2024.04.006

SUMMARY

Leprosy, one of the oldest recorded diseases in human history, remains prevalent in Asia, Africa, and South America, with over 200,000 cases every year.[1,2] Although ancient DNA (aDNA) approaches on the major causative agent, *Mycobacterium leprae,* have elucidated the disease's evolutionary history,[3–5] the role of animal hosts and interspecies transmission in the past remains unexplored. Research has uncovered relationships between medieval strains isolated from archaeological human remains and modern animal hosts such as the red squirrel in England.[6,7] However, the time frame, distribution, and direction of transmissions remains unknown. Here, we studied 25 human and 12 squirrel samples from two archaeological sites in Winchester, a medieval English city well known for its leprosarium and connections to the fur trade. We reconstructed four medieval *M. leprae* genomes, including one from a red squirrel, at a 2.2-fold average coverage. Our analysis revealed a phylogenetic placement of all strains on branch 3 as well as a close relationship between the squirrel strain and one newly reconstructed medieval human strain. In particular, the medieval squirrel strain is more closely related to some medieval human strains from Winchester than to modern red squirrel strains from England, indicating a yet-undetected circulation of *M. leprae* in non-human hosts in the Middle Ages. Our study represents the first One Health approach for *M. leprae* in archaeology, which is centered around a medieval animal host strain, and highlights the future capability of such approaches to understand the disease's zoonotic past and current potential.

RESULTS AND DISCUSSION

During the COVID-19 pandemic, the zoonotic potential of both new and millennia-old re-emerging infectious diseases and their multidrug resistance took center stage in modern society.[1,8–15] This calls for the development of new perspectives and scientific tools for disease characterization, prediction, and eradication. Interdisciplinary and collaborative approaches, such as One Health studies,[16] have come to the forefront to better understand disease dynamics and the complexity of factors that lead to adverse health outcomes.

Although zoonotic diseases have become increasingly prominent in modern health agendas, historical zoonoses have received scant attention, despite the potential importance of earlier transmission events in shaping past and present health landscapes.[17,18] Essential in the evolution and persistence of zoonotic pathogens are animal hosts,[19] which have been largely omitted from most studies on past diseases due to the lack of pathological and genetic research on zooarchaeological remains.[20] Without full pathogen genomes from archaeological animals, our understanding of long-term disease dynamics and animal-pathogen-human-environment interactions is hindered, as these are essential for contextualizing current trends and identifying potential spillover or reemergence risks.

Leprosy is mainly caused by *M. leprae* and to a lesser extent by *M. lepromatosis* and can lead to chronic infection, nerve

Figure 1. Location of the leprosarium of St Mary Magdalen and Staple Gardens in Winchester (center circle), within the UK

Top right shows Antiochus IV Epiphanes wearing a tunic lined with vair (squirrel fur, with the backs and fronts laid out in a checked pattern) in a 12th century Bible (Bibliothèque municipal de Dijon, MS 14 f. 191). Bottom right shows the three human samples that tested positive for *M. leprae*. Top left shows red squirrel sample bone SGW_S3_1, a right fourth metatarsal from Staple Gardens that tested positive for *M. leprae*. Bottom left shows a red squirrel in a 15th century Book of Hours (Bibliothèque de l'Arsenal, MS 5088 réserve, f. 175v).

damage, blindness, anosmia, alopecia, and dry skin in humans.[21] Left untreated, it can cause various distinctive and impairing lesions, making it a frequently described disease in historical sources.[22–24] Humans are the main host for both agents, though *M. leprae* does infect wild armadillos in the Americas and wild chimpanzees in West Africa, and both agents have been found in British red squirrels from Brownsea Island.[5,6,25,26] These modern red squirrels harbor a medieval *M. leprae* strain, insinuating a historic transmission event.[6] Even today, however, the mode of transmission between people, let alone the mode and direction of transmission between different potential animal hosts, is poorly understood. As an obligate intracellular pathogen, survival outside a host is unlikely, making the coexistence of animal and human hosts a likely factor in leprosy persistence. *M. leprae* has also been found in soil and water, suggesting a possible environmental component in the chain of transmission, though specifics remain unknown.[27] A better understanding of the significance, type, and contribution of all hosts in transmission is essential in leprosy eradication.[2,28] This, combined with potential historic interspecies transmission, makes leprosy an excellent focus for a first deep-time One Health pilot study. We present such a One Health approach by studying the historic and archaeological context of ancient cases of leprosy in humans and squirrels. We reconstruct four medieval *M. leprae* genomes, including a 2.2-fold average coverage genome isolated from a red squirrel bone, and contextualize them with ancient and modern data to decipher possible modes of transmission in medieval England and potential risk factors for transmission and evolution in this animal host today.

Opportunities for transmission in the medieval era

Extensive opportunities for transmission between humans and squirrels in the Middle Ages are visible in historic sources on the fur trade and petkeeping. Squirrel fur was by far the most widely used fur to trim and line garments in the High and Late Middle Ages.[29,30] In England, most of the skins came from Scandinavia, the Baltic, Eastern Europe, and Russia, along with Ireland, Scotland, and Italy. Squirrels would be trapped in the wild throughout the year and the skins would be transported for trade. Staggering quantities of squirrel skins were imported: for example, the English exchequer customs accounts for 1384 record 377,200 imported squirrel skins (with all other animal skins totaling less than 15,000). Vair, a way of laying out the backs and bellies of squirrel skins in a checked pattern (Figure 1), even became a heraldic tincture because it was so widely used in clothing.[31] Medieval iconography is replete with individuals wearing garments lined with squirrel fur.[32] Squirrels were also widely kept as pets. The practice is detailed in various sources, from records of episcopal visitations to the purchase of collars and leashes and the collared pet squirrels that abound in the margins of manuscripts.[33] Squirrels intended as pets were captured in the wild as kits and raised close to humans, often sitting on laps or shoulders.[34]

Table 1. Read-alignment results for all four *M. leprae*-positive samples

Sample	MMW_H50_1	MMW_H80_1	MMW_H94_1	SGW_S3_1	
Pre-processed reads	3041787	6979769	1657385	261511330	
Alignment algorithm	Bowtie2	Bowtie2	Bowtie2	Bowtie2	BWA
Mapped unique reads	556498	3828422	1375198	97072	37197
Average coverage	12.3×	86.2×	31.1×	2.2×	0.8×
1× covered (%)	97.8	100	99.8	52.0	44.3
3× covered (%)	87.9	100	98.6	10.2	3.6
5× covered (%)	75.6	99.9	95.8	5.1	0.5
Avg. fragment length (nt)	72.5	73.6	73.8	72.7	69.9
Radiocarbon dating (calCE)	1265–1377	991–1123	1176–1270	897–1025	

The table lists all reads passing the pre-processing step; the alignment algorithm; all unique reads aligned to the *M. leprae* reference genome; the average reference coverage; the percent of the reference, which is at least 1×, 3×, or 5× covered; the average fragment length of unique aligned reads; and the results for the 95.4% confidence interval of the calibrated radiocarbon dating. Since the bone from sample SGW_S3_1 has been used up completely for the DNA extraction, a cat bone from the same furrier pit has been dated. See also Figure S2 and Table S3.

To reflect these opportunities for transmission, we chose Winchester, an important medieval city with connections to key trading routes, for our study. Historic records show that skinners were active in Winchester preparing and selling a wide variety of fur-lined garments. Records for 1417 attest the presence of a "skinners row" on Winchester's High Street consisting of five stalls of skinners and one tailor's stall.[35] A number of archaeological sites have been associated with animal fur processing, including squirrel fur.[36–38] One context is the furrier pit in Staple Gardens, from which squirrel bones were analyzed for this study (Figure 1). Moreover, the site of St Mary Magdalen in Winchester represents one of the best-studied leprosaria in the UK, with confirmed molecular evidence of *M. leprae* including four recovered *M. leprae* genomes from human remains.[5,39] As such, Winchester is an ideal location to assess potential transmission of *M. leprae* between humans and squirrels.

Identification of potential human and squirrel leprosy cases from medieval Winchester

St Mary Magdalen's leprosarium offered remedial and palliative care to leprosy patients between the early 11th and late 15th centuries.[40,41] Many individuals buried at St Mary's have leprosy-associated lesions (78.5% for the earlier phase, 41.4% for the later phase, and 17.6% for the chapel).[42,43] Several individuals with leprosy-related lesions have been genetically tested in previous studies.[39,44–47] This study has focused on pathologically probable, non-characteristic, and non-pathological cases from burials unearthed in later field seasons. Multiple samples were taken from 11 individuals (Table S1). All samples were fully photographed prior to and after sampling, and pathological bone lesions were avoided when possible. See STAR Methods for a more in-depth site and skeleton description.

Less than two miles to the west, in the city center, lies Staple Gardens (Figure 1). This historic street dates to the 12th century and had at least one furrier shop between the 11th and 13th centuries. At this property, two pits containing a number of foot bones from cat, fox, squirrel, ferret/polecat, stoat, and unidentified small mammals were found. This pattern is typical of fur trading activities, as hands and feet often remained attached to the fur and were later removed in processing or were cut off first so that skin could be peeled off as a cone.[48,49] It remains unclear if and how squirrels would present osteological lesions due to *M. leprae* infection, though the lesions are likely to resemble those in humans.[50] Assuming the same low prevalence rate for skeletal lesions in squirrels as in humans (3%–5%), we focused on sampling bones with evidence for inflammation in the form of periosteal reactions (Figure S1) and sampled several bones without skeletal lesions. Twelve hand and foot bones (Table S1) from the largest furrier pit from Staple Gardens were sampled for ancient DNA (aDNA) extraction. These remains were randomly numbered, and all elements were photographed prior to sampling. More information on this site and the squirrel remains are in the STAR Methods and Table S1.

Analysis of the genetic data from medieval human and squirrel leprosy cases

Host DNA preservation and genetic evidence of *M. leprae* infection were assessed for all 25 human and 12 putative Eurasian red squirrel samples from Winchester using shotgun sequencing data (Table S2). Human samples with at least 2,000 reads mapping to the *M. leprae* reference and at least 10 reads mapping to the *M. leprae* specific repetitive RLEP region were used for targeted whole-genome enrichment. Only one Eurasian red squirrel sample had reads (two) mapping to the RLEP region. The shotgun data of this sample also showed more than 2,000 reads mapping to the complete *M. leprae* reference, and the sample was therefore selected for full genome enrichment (Table S3).

The squirrel bones originate from a furrier pit, which has been stratigraphically dated.[51] The dating was confirmed by radiocarbon dating a cat bone from the same context (Table 1; Figure S2C). As the pit contained bones from different small animal species, we used shotgun data from all putative squirrel samples to confirm the most probable species of sample origin. This was done by mapping reads against mitochondrial references representative of osteologically identified small animal species from the same excavation site (Figure 3C; Table S2). For all squirrel samples, *S. vulgaris* was confirmed as the most likely species.

Potentially positive samples were enriched for *M. leprae* fragments using a myBaits v4 in-solution hybridization approach. The squirrel libraries were also enriched using KAPA HyperExplore to overcome a potential enrichment bias and to maximize genome coverage. Of the two approaches, KAPA

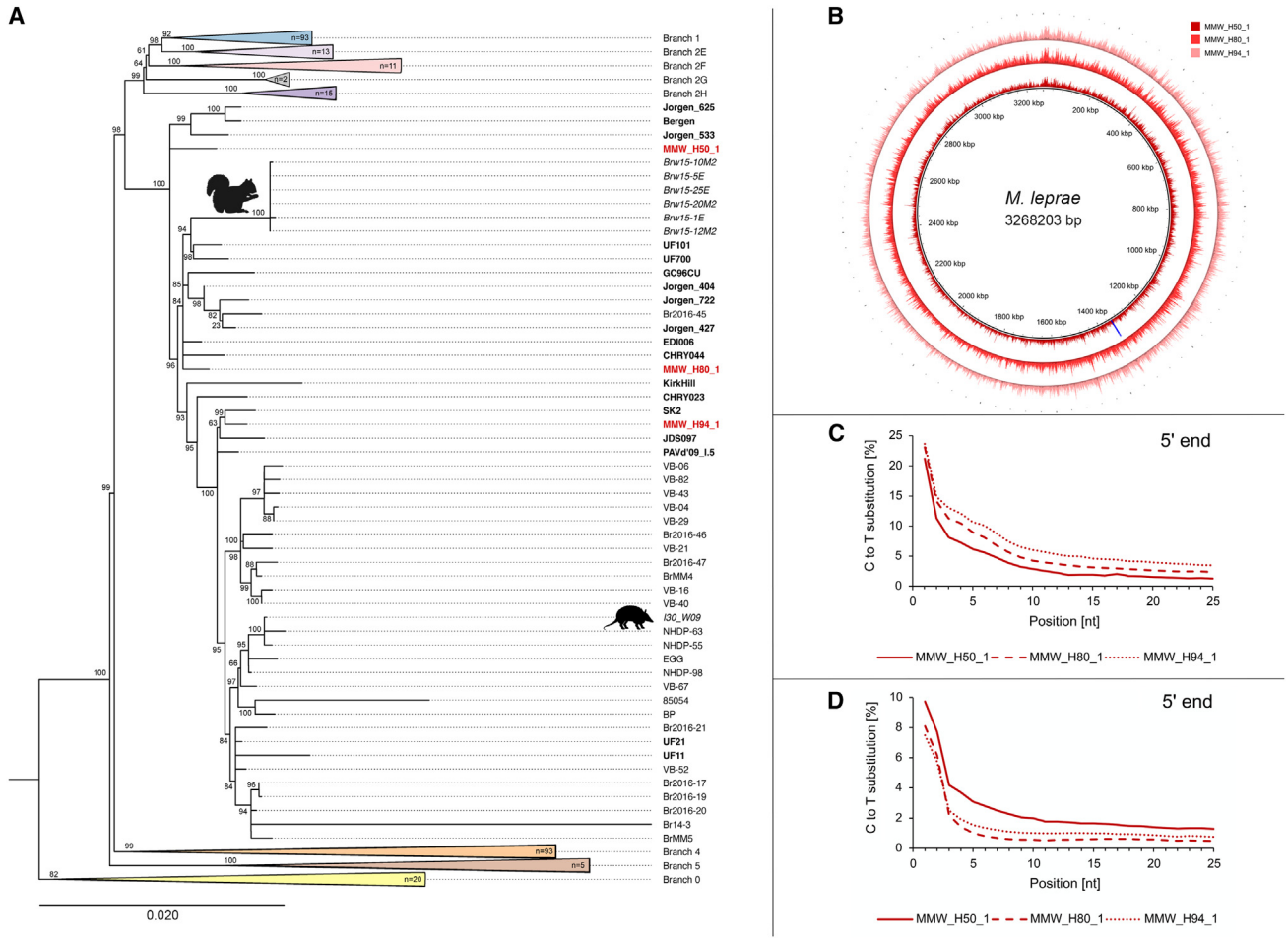

Figure 2. Genetic analysis of the three human skeletons of the leprosarium St. Mary Magdalen

(A) Collapsed maximum likelihood phylogenetic tree for *M. leprae* obtained using the whole-genome alignment. The tree is drawn to scale, with branch lengths measured in the number of substitutions per site. The three newly added ancient genomes are highlighted in bold red; previously published ancient genomes[3,5,53] of branch 3 are in bold; previously published genomes isolated from modern animal host[6,7] are in italic and include animal icons. The other branches are collapsed (*n* represents the number of included genomes) and are color-coded as follows: yellow for branch 0, brown for branch 5, orange for branch 4, purple for branch 2H, gray for branch 2G, pink for branch 2F, light purple for branch 2E, and blue for branch 1. See also Table S6.

(B) Circular coverage plots of the three *M. leprae* genomes isolated from MMW_H50_1 (dark red), MMW_H80_1 (red), and MMW_H94_1 (light red). Circles indicate genomic position and associated coverage (color dependent on the depicted genome). See also Table S3.

(C) DNA damage pattern plots at the 5′ end for the fragments mapping to the complete human reference genome (GRCh38.p14). See also Table S2.

(D) DNA damage pattern plots at the 5′ end for DNA fragments mapping to the *M. leprae* reference genome (GenBank: NC_002677.1). See also Table S3.

HyperExplore resulted in higher enrichment efficiency. All squirrel data were then combined and used for the final analyses. Data from *M. leprae* genome enrichment, using Bowtie2 alignment, resulted in the reconstruction of three complete *M. leprae* genomes from human samples (Table 1; Figure 2B) and a low-coverage genome from a squirrel bone (Table 1; Figure S2A). The human samples were radiocarbon dated (Figure S2C) and an aDNA characteristic deamination pattern[52] was assessed by mapping reads to *M. leprae* and host references (Figures 2C, 2D, 3D, and S2D; Tables S2 and S3). The coverage plot for the squirrel sample—potentially due to the low abundance of *M. leprae* fragments in the libraries—revealed several high coverage peaks (Figure S2A). These coverage spikes could stem from misalignments of environmental background to the reference. Therefore, we also applied stricter mapping parameters (Burrows-Wheeler Aligner: BWA, maximum edit distance of 0.2, mapping quality 37), resulting in a lower but more uniform coverage (Figure 3A). However, stricter mapping parameters could result in the false exclusion of authentic *M. leprae* reads due to mismatches caused by aDNA-associated-damage patterns. Therefore, all following analyses were carried out with both alignment algorithms, and results were compared. As an additional validation, reads from the enriched *M. leprae*-positive squirrel sample were mapped against an *M. leprae*-specific RLEP reference. RLEP is a repetitive element in the *M. leprae* genome and should therefore result in higher average coverage. The mapping showed at least 25× average coverage for both mapping algorithms (Table S3).

Data from the three human samples and the squirrel sample mapping to the full *M. leprae* TN reference genome

CellPress
OPEN ACCESS

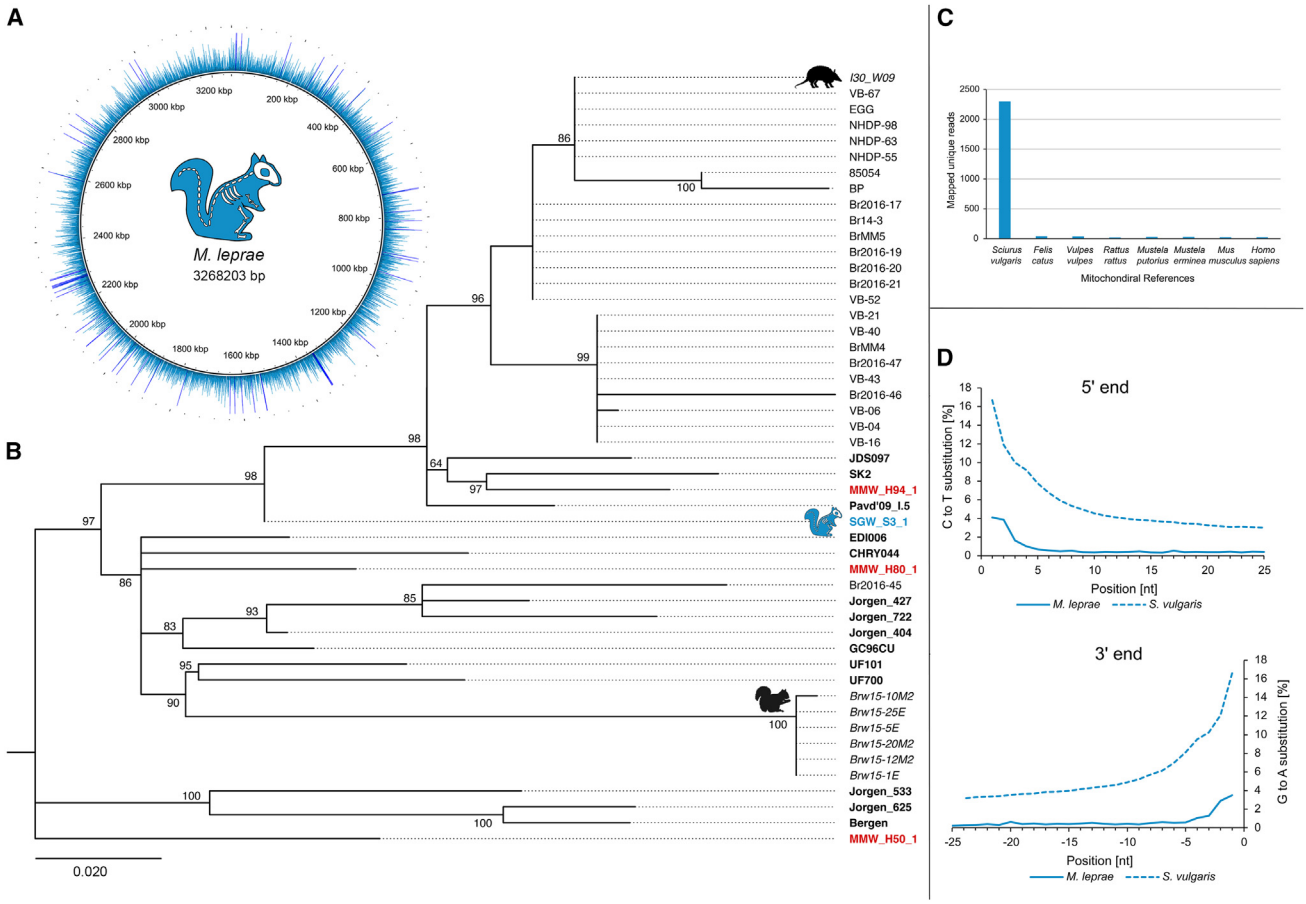

Figure 3. Genetic analysis of the squirrel bone from Staple Gardens

(A) Circular coverage plots of the *M. leprae* genome isolated from SGW_3_1 based on the stricter BWA alignment algorithm. Circles indicate genomic position and associated coverage (blue). See also Table S3.

(B) Maximum likelihood phylogenetic tree for *M. leprae* genomes of branch 3. The tree is drawn to scale, with branch lengths measured in the number of substitutions per site. The new ancient squirrel strain is highlighted in blue, bold and with an animal icon; the three new human strains are labeled in red and bold; previously published ancient genomes[3,5,53] of branch 3 are in bold; previously published genomes isolated from modern animal hosts[6,7] are in italic and include animal icons. Since only informative SNP positions identified in other samples were used to place the squirrel strain, it has no branch length. See also Table S5.

(C) Comparison of DNA fragments mapping to various host mitochondrial genomes (*Felis catus*, *Mustela erminea*, *Mustela putorius voucher*, *Sciurus vulgaris*, *Vulpes vulpes*, *Mus musculus*, *Rattus rattus*, and *Homo sapiens*). See also Table S2.

(D) DNA damage pattern plots at the 5′ end and 3′ end for DNA fragments mapping to the *M. leprae* reference genome (GenBank: NC_002677.1) based on the stricter BWA alignment algorithm and the *S. vulgaris* reference genome (GCA_902686455.2).[54] See also Tables S2 and S3.

(GenBank: NC_002677.1) were analyzed for specific SNP combinations to determine the genotype for each strain as described by Monot and colleagues.[55] The analysis was performed using the regular Bowtie2 alignment and the stricter BWA alignment. All four strains belong to branch 3 and specifically to genotype 3I (Table S4). To get deeper resolution in the newly sequenced ancient *M. leprae* strains, we used additional markers described by Truman and colleagues.[7] Due to the higher coverage, the human strains could be further resolved to SNP subtype 3I-1. The squirrel strain (SGW_S3_1) could not be further resolved because the required SNP156948 position was not covered (Table S5). One discrepancy was identified for the SNP typing at the position 1104232 (C instead of a G expected for the SNP type 3I). However, SGW_S3_1 shows a T at the position 7614, one copy of the indel_17915, and genotype 3I markers (Table S4), confirming the SNP subtype 3I.[7,55]

After the initial SNP-based placement of all four strains, we performed a phylogenetic analysis. The three human strains belong to branch 3, the most prominent branch for medieval European *M. leprae* genomes (Figure 2A; Table S6). Sample MMW_H94_1 clusters closely with SK2, a previously reconstructed *M. leprae* genome from human remains from the same leprosarium in Winchester.[5] The other strains from this leprosarium do not cluster closely together, which is in keeping with previously published evidence of high intra-leprosaria diversity.[3] The squirrel strain (SGW_S3_1) could not be used for our standard phylogeny analysis due to the low coverage. Therefore, informative SNPs were selected based on well-covered published branch 3 genomes and the three new human medieval genomes. A total of 299 positions were then used for genotyping (Table S5) by checking each position manually in Integrative Genomics Viewer (IGV).[56] After manual inspection, SNPs on

these 299 positions were used for phylogenetic placement of SGW_S3_1. The analysis was performed using the Bowtie2 alignment (Figure S2B) and the stricter BWA alignment (Figure 3B). To rule out any incorrect SNP calling based on aDNA characteristic deamination patterns,[52] analyses were re-run using mappings from both algorithms and truncated reads (both-sided truncation: 1 nt to 4 nt). In all cases, SGW_S3_1 falls in branch 3 and branches off basal to most modern human branch 3 genomes, the modern armadillo I30_W09, and medieval human strains, including two *M. leprae* genomes recovered from human remains from Winchester (MMW_H94_1 and SK2). Although SGW_S3_1 and modern *M. leprae* strains found in British *S. vulgaris*[6] all fall in branch 3, they do not cluster together, indicating independent transmission events.

In this study, we have taken the first step to a deep-time One Health approach to leprosy by combining multiple lines of evidence from historic sources, archaeological material, and aDNA analysis to showcase the presence of *M. leprae* strains belonging to the same genotype in medieval human and squirrel samples from Winchester. With historical records and archaeological data, we could find support for the presence of contemporaneous "risk factors" for possible interspecies *M. leprae* transmission, including red squirrel fur processing and trade within Winchester, while identifying new potential animal and human cases using paleopathological principles. In the genetic analysis, we could then reconstruct four new *M. leprae* genomes from three humans and one Eurasian red squirrel. Despite the low coverage of the squirrel *M. leprae* genome, which made additional tests for the robustness of our results necessary, we could confirm that the squirrel *M. leprae* genome diverges ancestrally from two human cases from Winchester. With all genomes clustering in branch 3, they represent the most prevalent leprosy strain type so far identified in medieval Britain,[3,5] and its presence in both species from the same city and time suggests cross-species infection.

As such, this study has identified the first historic *M. leprae* animal host and has successfully shown the presence of *M. leprae* in a red squirrel outside of Brownsea Island. However, the origin of infection in medieval red squirrels, and its contribution to transmission to humans, remains unclear. Animals could have been infected by humans[28] or by a yet-undetected animal or environmental reservoir in England.[19] Considering modern metadata with wild armadillos, close contact with infected living or dead animals represents a high risk of acquiring the disease for humans.[7,57] Our study identified circumstances and environments in which past transmission may have occurred, and in which cases of animal and human infection could thus be found. These findings substantiate the possibility of historic transmission events between humans and animals, which has previously only been indirectly suggested through identification of a historic strain in modern hosts.[5,58,59] Finding *M. leprae* DNA in archaeological animal remains represents the only direct source of evidence for past animal hosts, and additional *M. leprae* genomes from such animal hosts will be essential to further advance our understanding of the diversity of strains circulating in animal hosts and the frequency and direction of interspecies transmissions (human, animal, or environmental) in the past. Moreover, the successful reconstruction of a partial *M. leprae* genome from a squirrel metatarsal is a promising result for the future analysis of small non-articulated animal remains from archaeological contexts, which are often ignored.

This research, along with recent findings of leprosy in modern wild armadillos in the Americas,[25] wild red squirrels in the UK,[6,60,61] and potential insect vectors,[62,63] could open the medical debate to more seriously consider the possible role of animal hosts in leprosy persistence today. Understanding the distribution of the pathogen in historic host species can help us understand the evolutionary history of the disease, identify spillover risk factors both in the past and present, and advise modern public health strategies in regard to zoonotic reservoirs. Though this study represents a necessary step toward better understanding *M. leprae*'s transmission dynamics in different circumstances and times, more research is needed to fully map the coevolution of humans, animals, and their environment both in the past and today. Nevertheless, this study exemplifies how a multidisciplinary approach to an ancient disease can help target specific time periods, sites, and samples for *M. leprae* aDNA research while allowing the contextualization and explanation of results through past human behaviors. Research into both *M. leprae*'s evolution and host adaptations to the bacterium, alongside historic and archaeological research, is uniquely suited to help unravel when and why the disease jumped between species and to reconstruct, predict, and prevent such events for public health interest.

STAR★METHODS

Detailed methods are provided in the online version of this paper and include the following:

- KEY RESOURCES TABLE
- RESOURCE AVAILABILITY
  - Lead contact
  - Materials availability
  - Data and code availability
- EXPERIMENTAL MODEL AND SUBJECT DETAILS
  - Ethics
  - Human sample selection
  - Human remains: St Mary Magdalen, Winchester
  - Skeleton descriptions St Mary Magdalen Winchester
  - Squirrel remains: Staple Gardens, Winchester
  - Squirrel sample descriptions
- METHOD DETAILS
  - Human osteology and palaeopathology
  - Sampling and DNA extraction
  - Double-stranded library construction and double indexing
  - Shotgun sequencing
  - Initial *M. leprae* myBait full genome enrichment
  - Additional library preparation for SGW_3_1
  - Second *M. leprae* myBait full genome enrichment
  - HyperExplore bait capture of SGW_3_1 and data analysis
  - Collagen extraction (St Mary Magdalen, human samples)
  - Collagen extraction (furrier pit, animal sample)
  - Radiocarbon dating
- QUANTIFICATION AND STATISTICAL ANALYSIS
  - DNA preservation assessment for all Winchester samples
  - Shotgun data screening for potential *M. leprae* positive human and squirrel samples
  - Squirrel sample species verification
  - Data analysis of *M. leprae* enrichment (BWA)
  - Data analysis of *M. leprae* enrichment for human samples (Bowtie2)
  - SGW_3_1 read truncation for phylogenetic analysis
  - Genotyping of SGW_3_1 using partial genome sequencing

- Phylogenetic tree construction
- Coverage plots

SUPPLEMENTAL INFORMATION

Supplemental information can be found online at https://doi.org/10.1016/j.cub.2024.04.006.

ACKNOWLEDGMENTS

We would like to thank Irka Hajdas (ETH Zurich) for carrying out the 14C dating of this study, the Functional Genomics Center Zurich and the Next Generation Sequencing Facility of the Vienna Biocenter Core Facilities for sequencing, Corina Steiner and Stephan Symons for support with the figure design, and Lena Strid for her information regarding the squirrels at Winchester.

Many thanks to the Koninklijke Bibliotheek van België (KBR) for permission to reproduce KBR MS 10607 f. 88r for the graphical abstract.

This work was supported by the SERI-funded ERC Consolidator Grant "RESERVOIR" (grant no. MB23.00001 REF-1131-52105 to V.J.S.) and the University of Zurich's University Research Priority Program "Evolution in Action: From Genomes to Ecosystems" (V.J.S. and C.U.). C.A. was supported by the Fondation Raoul Follereau and the Heiser Program of the New York Community Trust for Research in Leprosy (grant no. P21–000127, C.A.).

AUTHOR CONTRIBUTIONS

V.J.S., S.A.I., C.U., A.A.B., and K.W.-M. conceived and designed the study. K.W.-I., R.T., P.M., H.D.-H., S.R., and S.A.I. provided samples and archaeological context. V.J.S. and S.A.I. supervised the work and provided funding. C.U., A.A.B., and C.A. performed the experimental work. C.U., A.A.B., C.A., and A.K.W. analyzed the generated data. C.U., A.A.B., V.J.S., S.A.I., K.W.-M., and C.A. wrote the manuscript with input from all authors. All authors reviewed the manuscript.

DECLARATION OF INTERESTS

We have no competing interests.

Received: October 13, 2023
Revised: February 15, 2024
Accepted: April 2, 2024
Published: May 3, 2024

REFERENCES

1. World Health Organization, Regional Office for South-East Asia (2016). Global Leprosy Strategy 2016-2020: Accelerating towards a leprosy-free world (WHO Regional Office for South-East Asia).
2. World Health Organization, Regional Office for South-East Asia (2020). Global consultation of National Leprosy Programme managers, partners and affected persons on Global Leprosy Strategy 2021–2030: Report of the virtual meeting 26-30 October 2020. 978-92-9022-822-6.
3. Pfrengle, S., Neukamm, J., Guellil, M., Keller, M., Molak, M., Avanzi, C., Kushniarevich, A., Montes, N., Neumann, G.U., Reiter, E., et al. (2021). Mycobacterium leprae diversity and population dynamics in medieval Europe from novel ancient genomes. BMC Biol. *19*, 220.
4. Neukamm, J., Pfrengle, S., Molak, M., Seitz, A., Francken, M., Eppenberger, P., Avanzi, C., Reiter, E., Urban, C., Welte, B., et al. (2020). 2000-year-old pathogen genomes reconstructed from metagenomic analysis of Egyptian mummified individuals. BMC Biol. *18*, 108.
5. Schuenemann, V.J., Singh, P., Mendum, T.A., Krause-Kyora, B., Jäger, G., Bos, K.I., Herbig, A., Economou, C., Benjak, A., Busso, P., et al. (2013). Genome-wide comparison of medieval and modern Mycobacterium leprae. Science *341*, 179–183.
6. Avanzi, C., Del-Pozo, J., Benjak, A., Stevenson, K., Simpson, V.R., Busso, P., McLuckie, J., Loiseau, C., Lawton, C., Schoening, J., et al. (2016). Red squirrels in the British Isles are infected with leprosy bacilli. Science *354*, 744–747.
7. Truman, R.W., Singh, P., Sharma, R., Busso, P., Rougemont, J., Paniz-Mondolfi, A., Kapopoulou, A., Brisse, S., Scollard, D.M., Gillis, T.P., and Cole, S.T. (2011). Probable zoonotic leprosy in the southern United States. N. Engl. J. Med. *364*, 1626–1633.
8. Wu, F., Zhao, S., Yu, B., Chen, Y.-M., Wang, W., Song, Z.-G., Hu, Y., Tao, Z.-W., Tian, J.-H., Pei, Y.-Y., et al. (2020). A new coronavirus associated with human respiratory disease in China. Nature *579*, 265–269.
9. Lam, T.T.-Y., Jia, N., Zhang, Y.-W., Shum, M.H.-H., Jiang, J.-F., Zhu, H.-C., Tong, Y.-G., Shi, Y.-X., Ni, X.-B., Liao, Y.-S., et al. (2020). Identifying SARS-CoV-2-related coronaviruses in Malayan pangolins. Nature *583*, 282–285.
10. Zhou, P., Yang, X.-L., Wang, X.-G., Hu, B., Zhang, L., Zhang, W., Si, H.-R., Zhu, Y., Li, B., Huang, C.-L., et al. (2020). Addendum: A pneumonia outbreak associated with a new coronavirus of probable bat origin. Nature *588*, E6.
11. Brennan, P.J. (1997). Tuberculosis in the context of emerging and reemerging diseases. FEMS Immunol. Med. Microbiol. *18*, 263–269.
12. World Health Organization (2022). Plague. https://www.who.int/news-room/fact-sheets/detail/plague.
13. Maeda, S., Matsuoka, M., Nakata, N., Kai, M., Maeda, Y., Hashimoto, K., Kimura, H., Kobayashi, K., and Kashiwabara, Y. (2001). Multidrug resistant Mycobacterium leprae from patients with leprosy. Antimicrob. Agents Chemother. *45*, 3635–3639.
14. World Health Organization (1993). Tuberculosis: a global emergency [full issue]. World Health *46*, 3–31.
15. Welch, T.J., Fricke, W.F., McDermott, P.F., White, D.G., Rosso, M.-L., Rasko, D.A., Mammel, M.K., Eppinger, M., Rosovitz, M.J., Wagner, D., et al. (2007). Multiple antimicrobial resistance in plague: an emerging public health risk. PLoS One *2*, e309.
16. One Health High-Level Expert Panel OHHLEP, Adisasmito, W.B., Almuhairi, S., Behravesh, C.B., Bilivogui, P., Bukachi, S.A., Casas, N., Cediel Becerra, N., Charron, D.F., Chaudhary, A., et al. (2022). One Health: A new definition for a sustainable and healthy future. PLoS Pathog. *18*, e1010537.
17. Wolfe, N.D., Dunavan, C.P., and Diamond, J. (2007). Origins of major human infectious diseases. Nature *447*, 279–283.
18. Plomp, K.A., Roberts, C.A., Elton, S., and Bentley, G.R. (2022). Palaeopathology and Evolutionary Medicine: An Integrated Approach (Oxford University Press).
19. Ploemacher, T., Faber, W.R., Menke, H., Rutten, V., and Pieters, T. (2020). Reservoirs and transmission routes of leprosy; A systematic review. PLoS Negl. Trop. Dis. *14*, e0008276.
20. Thomas, R. (2019). Chapter 23 - Nonhuman Animal Paleopathology—Are We so Different? In Ortner's Identification of Pathological Conditions in Human Skeletal Remains, Third Edition, J.E. Buikstra, ed. (Academic Press), pp. 809–822.
21. Kumar, B., Uprety, S., and Dogra, S. (2017). Clinical diagnosis of leprosy. International Textbook of Leprosy.
22. Van Brakel, W.H., Peters, R.M., Bakirtzief, Z., and Pereira, S. Stigma related to leprosy—A scientific view. https://www.internationaltextbookofleprosy.com/sites/default/files/ITL_4_5%20FINAL.pdf.
23. Jacob, J.T., and Franco-Paredes, C. (2008). The stigmatization of leprosy in India and its impact on future approaches to elimination and control. PLoS Negl. Trop. Dis. *2*, e113.
24. World Health Organization, Regional Office for South-East Asia (2018). Guidelines for the diagnosis, treatment and prevention of leprosy.
25. Deps, P., Antunes, J.M., Santos, A.R., and Collin, S.M. (2020). Prevalence of Mycobacterium leprae in armadillos in Brazil: A systematic review and meta-analysis. PLoS Negl. Trop. Dis. *14*, e0008127.
26. Hockings, K.J., Mubemba, B., Avanzi, C., Pleh, K., Düx, A., Bersacola, E., Bessa, J., Ramon, M., Metzger, S., Patrono, L.V., et al. (2021). Leprosy in wild chimpanzees. Nature *598*, 652–656.

27. Turankar, R.P., Lavania, M., Darlong, J., Siva Sai, K.S.R., Sengupta, U., and Jadhav, R.S. (2019). Survival of Mycobacterium leprae and association with Acanthamoeba from environmental samples in the inhabitant areas of active leprosy cases: A cross sectional study from endemic pockets of Purulia, West Bengal. Infect. Genet. Evol. *72*, 199–204.

28. Deps, P., and Rosa, P.S. (2021). One Health and Hansen's disease in Brazil. PLoS Negl. Trop. Dis. *15*, e0009398.

29. E. Ewing, ed. (1981). Fur in dress (Batsford).

30. Newton, S.M. (1999). Fashion in the Age of the Black Prince: A Study of the Years 1340-1365 (Boydell & Brewer).

31. Phoenix, D. (2010). "Garments so Chequered": the Bible of Cîteaux, the Bayeux Tapestry and the Vair Pattern. Antiq. J. *90*, 195–210.

32. Scott, M. (2009). Medieval Dress & Fashion (British Library).

33. Walker-Meikle, K. (2012). Medieval Pets (Boydell Press).

34. Topsell, E. (1658). The history of four-footed beasts and serpents (Printed by E. Cotes).

35. Deering, C.L. (2014). Cluster and Clash? Everyday Space and the Butchers of Late Medieval Winchester, C. 1360-1420. (Thesis Ph.D.).

36. Teague, S. (2011). The medieval period (1050-1500). In Winchester - a City in the Making: Archaeological Excavations Between 2002 and 2007 on the Sites of Northgate House, Staple Gardens and the Former Winchester Library, Jewry St, B.M. Ford, and S. Teague, eds. (Oxford Archaeology).

37. Teague, S. (2011). The Anglo-Saxon Burh, and the Anglo-Norman and medieval city: overview and discussion of the evidence. In Winchester - a City in the Making: Archaeological Excavations Between 2002 and 2007 on the Sites of Northgate House, Staple Gardens and the Former Winchester Library, J. St, B.M. Ford, and S. Teague, eds. (Oxford Archaeology).

38. Serjeantson, D., and Rees, H. (2009). Food, Craft and Status in Medieval Winchester: The Plant and Animal Remains from the Suburbs and City Defences (Winchester Museums).

39. Mendum, T.A., Schuenemann, V.J., Roffey, S., Taylor, G.M., Wu, H., Singh, P., Tucker, K., Hinds, J., Cole, S.T., Kierzek, A.M., et al. (2014). Mycobacterium leprae genomes from a British medieval leprosy hospital: towards understanding an ancient epidemic. BMC Genom. *15*, 270.

40. Roffey, S., and Tucker, K. (2012). A contextual study of the medieval hospital and cemetery of St Mary Magdalen, Winchester, England. Int. J. Paleopathol. *2*, 170–180.

41. Roffey, S. (2020). Sanctity and Suffering: The Sacred World of the Medieval Leprosarium. A Perspective from St Mary Magdalen, Winchester. In The Land of the English Kin (Brill), pp. 538–554.

42. Roffey, S. (2012). Medieval Leper Hospitals in England: An Archaeological Perspective. Mediev. Archaeol. *56*, 203–233.

43. Tucker, K. (2018). Analysis of the inhumations and disarticulated human bone from excavations at St. Mary Magdalen leprosy hospital. Winchester (University of Winchester 2009-2012, 2015; Time Team 2000) University of Winchester. (Unpublished report).

44. Taylor, G.M., White-Iribhogbe, K., Cole, G., Ashby, D., Stewart, G.R., and Dawson-Hobbis, H. (2024). Bioarchaeological investigation of individuals with suspected multibacillary leprosy from the mediaeval leprosarium of St Mary Magdalen, Winchester, Hampshire, UK. J. Med. Microbiol. *73*, https://doi.org/10.1099/jmm.0.001806.

45. Taylor, G.M., Tucker, K., Butler, R., Pike, A.W.G., Lewis, J., Roffey, S., Marter, P., Lee, O.Y.-C., Wu, H.H.T., Minnikin, D.E., et al. (2013). Detection and strain typing of ancient Mycobacterium leprae from a medieval leprosy hospital. PLoS One *8*, e62406.

46. Roffey, S., Tucker, K., Filipek-Ogden, K., Montgomery, J., Cameron, J., O'Connell, T., Evans, J., Marter, P., and Taylor, G.M. (2017). Investigation of a Medieval Pilgrim Burial Excavated from the Leprosarium of St Mary Magdalen Winchester, UK. PLoS Negl. Trop. Dis. *11*, e0005186.

47. Cole, G., Taylor, G.M., Stewart, G.R., and Dawson-Hobbis, H. (2022). Ancient DNA confirmation of lepromatous leprosy in a skeleton with concurrent osteosarcoma, excavated from the leprosarium of St. Mary Magdalen in Winchester, Hants., UK. Eur. J. Clin. Microbiol. Infect. Dis. *41*, 1295–1304.

48. Fairnell, E.H. (2003). The Utilisation of Fur-bearing Animals in the British Isles: A Zooarchaeological Hunt for Data. https://www.fairnell.co.uk/content/documents/eva-fairnell-msc-thesis.pdf.

49. Fairnell, E.H. (2008). 101 ways to skin a fur-bearing animal: the implications for zooarchaeological interpretation. In Experiencing Archaeology by Experiment, P. Cunningham, J. Heeb, and R. Paardekooper, eds. (Oxbow Books), p. 13.

50. Urban, C., Blom, A.A., Pfrengle, S., Walker-Meikle, K., Stone, A.C., Inskip, S.A., and Schuenemann, V.J. (2021). One health approaches to trace Mycobacterium leprae's zoonotic potential through time. Front. Microbiol. *12*, 762263.

51. Griffiths, S., Bayliss, A., Ford, B., Hounslow, M., Karkoukovski, M., Bronk Ramsey, C., Cook, G., and Marhsall, P. (2011). Scientific dating and chronology. In Winchester - a City in the Making: Archaeological Excavations Between 2002 and 2007 on the Sites of Northgate House, Staple Gardens and the Former Winchester Library, Jewry St (Oxford Archaeology).

52. Sawyer, S., Krause, J., Guschanski, K., Savolainen, V., and Pääbo, S. (2012). Temporal patterns of nucleotide misincorporations and DNA fragmentation in ancient DNA. PLoS One *7*, e34131.

53. Schuenemann, V.J., Avanzi, C., Krause-Kyora, B., Seitz, A., Herbig, A., Inskip, S., Bonazzi, M., Reiter, E., Urban, C., Dangvard Pedersen, D., et al. (2018). Ancient genomes reveal a high diversity of Mycobacterium leprae in medieval Europe. PLoS Pathog. *14*, e1006997.

54. Mead, D., Fingland, K., Cripps, R., Portela Miguez, R., Smith, M., Corton, C., Oliver, K., Skelton, J., Betteridge, E., Doucan, J., et al. (2020). The genome sequence of the Eurasian red squirrel, Sciurus vulgaris Linnaeus 1758. Wellcome Open Res. *5*, 18.

55. Monot, M., Honoré, N., Garnier, T., Zidane, N., Sherafi, D., Paniz-Mondolfi, A., Matsuoka, M., Michael Taylor, G., Donoghue, H.D., Bouwman, A., et al. (2009). Comparative genomic and phylogeographic analysis of Mycobacterium leprae. Preprint. https://doi.org/10.1038/ng.477.

56. Robinson, J.T., Thorvaldsdóttir, H., Wenger, A.M., Zehir, A., and Mesirov, J.P. (2017). Variant Review with the Integrative Genomics Viewer. Cancer Res. *77*, e31–e34.

57. da Silva, M.B., Portela, J.M., Li, W., Jackson, M., Gonzalez-Juarrero, M., Hidalgo, A.S., Belisle, J.T., Bouth, R.C., Gobbo, A.R., Barreto, J.G., et al. (2018). Evidence of zoonotic leprosy in Pará, Brazilian Amazon, and risks associated with human contact or consumption of armadillos. PLoS Negl. Trop. Dis. *12*, e0006532.

58. Monot, M., Honoré, N., Garnier, T., Araoz, R., Coppée, J.Y., Lacroix, C., Sow, S., Spencer, J.S., Truman, R.W., Williams, D.L., et al. (2005). On the origin of leprosy. Science *308*, 1040–1042.

59. Inskip, S., Taylor, G.M., Anderson, S., and Stewart, G. (2017). Leprosy in pre-Norman Suffolk, UK: biomolecular and geochemical analysis of the woman from Hoxne. J. Med. Microbiol. *66*, 1640–1649.

60. Meredith, A., Del Pozo, J., Smith, S., Milne, E., Stevenson, K., and McLuckie, J. (2014). Leprosy in red squirrels in Scotland. Vet. Rec. *175*, 285–286.

61. Simpson, V., Hargreaves, J., Butler, H., Blackett, T., Stevenson, K., and McLuckie, J. (2015). Leprosy in red squirrels on the Isle of Wight and Brownsea Island. Vet. Rec. *177*, 206–207.

62. Ferreira, J.d.S., Souza Oliveira, D.A., Santos, J.P., Ribeiro, C.C.D.U., Baêta, B.A., Teixeira, R.C., Neumann, A.d.S., Rosa, P.S., Pessolani, M.C.V., Moraes, M.O., et al. (2018). Ticks as potential vectors of Mycobacterium leprae: Use of tick cell lines to culture the bacilli and generate transgenic strains. PLoS Negl. Trop. Dis. *12*, e0007001.

63. Tongluan, N., Shelton, L.T., Collins, J.H., Ingraffia, P., McCormick, G., Pena, M., Sharma, R., Lahiri, R., Adams, L.B., Truman, R.W., and

Macaluso, K.R. (2021). Mycobacterium leprae Infection in Ticks and Tick-Derived Cells. Front. Microbiol. *12*, 761420.

64. Meyer, M., and Kircher, M. (2010). Illumina sequencing library preparation for highly multiplexed target capture and sequencing. Cold Spring Harb. Protoc. *2010*. pdb.prot5448.
65. Peltzer, A., Jäger, G., Herbig, A., Seitz, A., Kniep, C., Krause, J., and Nieselt, K. (2016). EAGER: efficient ancient genome reconstruction. Genome Biol. *17*, 60.
66. Andrews, S. (2010). FastQC: a quality control tool for high throughput sequence data.
67. Schubert, M., Lindgreen, S., and Orlando, L. (2016). AdapterRemoval v2: rapid adapter trimming, identification, and read merging. BMC Res. Notes *9*, 88.
68. Li, H., and Durbin, R. (2009). Fast and accurate short read alignment with Burrows-Wheeler transform. Bioinformatics *25*, 1754–1760.
69. Broad Institute (2017). Picard tools. https://github.com/broadinstitute/picard/releases.
70. Neukamm, J., Peltzer, A., and Nieselt, K. (2021). DamageProfiler: fast damage pattern calculation for ancient DNA. Bioinformatics *37*, 3652–3653.
71. Langmead, B., and Salzberg, S.L. (2012). Fast gapped-read alignment with Bowtie 2. Nat. Methods *9*, 357–359.
72. Bolger, A.M., Lohse, M., and Usadel, B. (2014). Trimmomatic: a flexible trimmer for Illumina sequence data. Bioinformatics *30*, 2114–2120.
73. Koboldt, D.C., Zhang, Q., Larson, D.E., Shen, D., McLellan, M.D., Lin, L., Miller, C.A., Mardis, E.R., Ding, L., and Wilson, R.K. (2012). VarScan 2: somatic mutation and copy number alteration discovery in cancer by exome sequencing. Genome Res. *22*, 568–576.
74. Cingolani, P., Platts, A., Wang, L.L., Coon, M., Nguyen, T., Wang, L., Land, S.J., Lu, X., and Ruden, D.M. (2012). A program for annotating and predicting the effects of single nucleotide polymorphisms, SnpEff: SNPs in the genome of Drosophila melanogaster strain w1118; iso-2; iso-3. Fly *6*, 80–92.
75. Chen, S., Zhou, Y., Chen, Y., and Gu, J. (2018). fastp: an ultra-fast all-in-one FASTQ preprocessor. Bioinformatics *34*, i884–i890.
76. Alikhan, N.-F., Petty, N.K., Ben Zakour, N.L., and Beatson, S.A. (2011). BLAST Ring Image Generator (BRIG): simple prokaryote genome comparisons. BMC Genom. *12*, 402.
77. Kumar, S., Stecher, G., Li, M., Knyaz, C., and Tamura, K. (2018). MEGA X: Molecular Evolutionary Genetics Analysis across Computing Platforms. Mol. Biol. Evol. *35*, 1547–1549.
78. Barlow, F. (1979). The Winton Domesday. In Winchester in the early Middle Ages: An edition and discussion of the Winton Domesday, F. Barlow, M. Biddle, O.v. Feilitzen, and D.J. Keene, eds. (Clarendon Press), pp. 1–144.
79. Doubleday, H.A., and Page, W. (1903). History of the County of Hampshire, *Volume 2* (HMSO).
80. Ford, B.M., and Allen, M. (2011). Winchester-a city in the making: archaeological excavations between 2002 and 2007 on the sites of Northgate House, Staple Gardens and the former Winchester Library, Jewry St (Oxford Archaeology).
81. Moore, H., and Preston, S. (2008). Late Saxon and Early Medieval occupation at 26-27 Staple Gardens,Winchester. Proc. Hampshire Fld. Club Archaeol. Soc. *63*, 135–178.
82. Martin, G., and Priestley, S. (2010). Programme of archaeological work at staple chambers staple gardens Winchester Hampshire (Archaeology Data Service). https://doi.org/10.5284/1082169.
83. Stird, L. (2011). Mammal and bird bones. In Winchester - a City in the Making: Archaeological Excavations Between 2002 and 2007 on the Sites of Northgate House, Staple Gardens and the Former Winchester Library, J. St, B.M. Ford, and S. Teague, eds. (Oxford Archaeology).
84. Mitchell, P.D., and Brickley, M. (2017). Updated guidelines to the standards for recording human remains (Chartered Institute for Archaeologists).
85. Møller-Christensen, V. (1978). Leprosy Changes of the Skull (Odense University Press).
86. Andersen, J.G., and Manchester, K. (1987). Grooving of the proximal phalanx in leprosy: A palaeopathological and radiological study. J. Archaeol. Sci. *14*, 77–82.
87. Andersen, J.G., and Manchester, K. (1992). The rhinomaxillary syndrome in leprosy: A clinical, radiological and palaeopathological study. Int. J. Osteoarchaeol. *2*, 121–129.
88. Andersen, J.G., Manchester, K., and Ali, R.S. (1992). Diaphyseal remodelling in leprosy: A radiological and palaeopathological study. Int. J. Osteoarchaeol. *2*, 211–219.
89. Andersen, J.G., Manchester, K., and Roberts, C. (1994). Septic bone changes in leprosy: A clinical, radiological and palaeopathological review. Int. J. Osteoarchaeol. *4*, 21–30.
90. Andersen, J.G., and Manchester, K. (1988). Dorsal tarsal exostoses in leprosy: A palaeopathological and radiological study. J. Archaeol. Sci. *15*, 51–56.
91. Lewis, M.E., Roberts, C.A., and Manchester, K. (1995). Inflammatory bone changes in leprous skeletons from the medieval Hospital of St. James and St. Mary Magdalene, Chichester, England. Int. J. Lepr. Other Mycobact. Dis. *63*, 77–85.
92. Manchester, K., and Roberts, C. (1989). The Palaeopathology of leprosy in Britain: A review. World Archaeol. *21*, 265–272.
93. Ortner, D.J. (2002). Observations on the pathogenesis of skeletal disease in leprosy. In The past and present of leprosy (archaeological, historical, palaeopathological and clinical approaches), pp. 73–80. pascal-francis.inist.fr.
94. Roberts, C.A. (2020). Leprosy: Past and Present (University of Florida Press).
95. Roberts, C. (2018). The bioarchaeology of leprosy: Learning from the past. https://internationaltextbookofleprosy.org/sites/default/files/ITL_11_1%20FINAL_0.pdf.
96. Roberts, C.A., and Buikstra, J.E. (2019). Chapter 11 - Bacterial Infections. In Ortner's Identification of Pathological Conditions in Human Skeletal Remains, Third Edition, J.E. Buikstra, ed. (Academic Press), pp. 321–439.
97. Manchester, K. (2002). Infective bones changes in leprosy. In The past and present of leprosy (archaeological, historical, palaeopathological and clinical approaches), pp. 69–72. pascal-francis.inist.fr.
98. Ortner, D.J. (2008). Skeletal manifestations of leprosy. In "Lepers Outside the Gate": Excavations at the Cemetery of the Hospital of St James and St Mary Magdalene, Chichester, 1986-87 and 1993, , J.R. Magilton, F. Lee, and A. Boylston, eds.
99. Cooper, A., and Poinar, H.N. (2000). Ancient DNA: do it right or not at all. Science *289*, 1139.
100. Dabney, J., and Meyer, M. (2019). Extraction of Highly Degraded DNA from Ancient Bones and Teeth. Methods Mol. Biol. *1963*, 25–29.
101. Kircher, M., Sawyer, S., and Meyer, M. (2012). Double indexing overcomes inaccuracies in multiplex sequencing on the Illumina platform. Nucleic Acids Res. *40*, e3.
102. Honap, T.P., Pfister, L.-A., Housman, G., Mills, S., Tarara, R.P., Suzuki, K., Cuozzo, F.P., Sauther, M.L., Rosenberg, M.S., and Stone, A.C. (2018). Mycobacterium leprae genomes from naturally infected nonhuman primates. PLoS Negl. Trop. Dis. *12*, 61900–e6217.
103. Longin, R. (1971). New method of collagen extraction for radiocarbon dating. Nature *230*, 241–242.
104. Privat, K.L. (1999). Stable isotope analysis of human and faunal remains from the anglo-saxon cemetery at Berinsfield. Oxfordshire: dietary and social implications (University of Sheffield, Department of Archaeology and Prehistory).

105. Hajdas, I., Michczyński, A., Bonani, G., Wacker, L., and Furrer, H. (2009). Dating Bones near the Limit of the Radiocarbon Dating Method: Study Case Mammoth from Niederweningen, ZH Switzerland. Radiocarbon *51*, 675–680.

106. Ramsey, C.B. (2017). Methods for summarizing radiocarbon datasets. Radiocarbon *59*, 1809–1833.

107. Reimer, P.J., Austin, W.E.N., Bard, E., Bayliss, A., Blackwell, P.G., Bronk Ramsey, C., Butzin, M., Cheng, H., Edwards, R.L., Friedrich, M., et al. (2020). The IntCal20 Northern Hemisphere Radiocarbon Age Calibration Curve (0–55 cal kBP). Radiocarbon *62*, 725–757.

108. Benjak, A., Avanzi, C., Singh, P., Loiseau, C., Girma, S., Busso, P., Fontes, A.N.B., Miyamoto, Y., Namisato, M., Bobosha, K., et al. (2018). Phylogenomics and antimicrobial resistance of the leprosy bacillus Mycobacterium leprae. Nat. Commun. *9*, 352.

109. Nei, M., and Kumar, S. (2000). Molecular Evolution and Phylogenetics (Oxford University Press).

110. Kimura, M. (1980). A simple method for estimating evolutionary rates of base substitutions through comparative studies of nucleotide sequences. J. Mol. Evol. *16*, 111–120.

STAR★METHODS

KEY RESOURCES TABLE

REAGENT or RESOURCE	SOURCE	IDENTIFIER
Biological samples		
Human archeological remains	This study	BioProject: PRJNA1021938, Table S1
Squirrel archeological remains	This study	BioProject: PRJNA1021938, Table S1
Chemicals, peptides, and recombinant proteins		
EDTA 0.5 M	AppliChem	Cat#A4892.1000
Proteinase K, 20 mg/mL	New England Biolabs	Cat#P8107S
UltraPure™ DNase/RNase-Free Distilled Water	Invitrogen	Cat#10977035
Guanidin hydrochlorid	Sigma-Aldrich	Cat#50950
2-Propanol	Sigma-Aldrich	Cat#I9516
Sodium Acetate, 3 M, pH 5.2	avantor	Cat#733-1634
Ethanol	Sigma-Aldrich	Cat#1.08543
Tris-HCl, 1 M, pH 8.0	Thermo Fischer Scientific	Cat#15568-025
BSA, 20 mg/mL	New England Biolabs	Cat#B9000S
ATP, 10 mM	New England Biolabs	Cat#P0756S
dNTP Mix (25 mM each)	Thermo Fischer Scientific	Cat#R1121
T4 Polynucleotide Kinase, 10 U/ul	New England Biolabs	Cat#M0201L
T4 DNA Polymerase, 3 U/μL	New England Biolabs	Cat#M0203S
Quick Ligation™ Kit	New England Biolabs	Cat#M2200L
Bst 2.0 DNA Polymerase	New England Biolabs	Cat#M0537L
PfuTurbo Cx Hotstart DNA Polymerase, 2.5 U/μL	Agilent	Cat#600414
Herculase II Fusion DNA Polymerase	Agilent	Cat#600679
SYBR™ Green PCR Master Mix, 2x	Thermo Fischer Scientific	Cat#4364344
Dynabeads™ MyOne™ Streptavidin C1	Thermo Fisher Scientific	Cat#65002
Tween 20	Sigma Aldrich	Cat#P9416
Critical commercial assays		
Zymo-Spin V Columns w/ Reservoir	Zymo Research	Cat#C1016-50
MinElute PCR Purification Kit	Qiagen	Cat#28004
D1000 ScreenTape	Agilent	Cat#5067-5582
D1000 Sample Buffer	Agilent	Cat#5067-5602
KAPA HyperExplore Max 3Mb	Roche	IRN 1000013073
myBaits v4	Arbor Biosciences	Design: 180220-90
Deposited data		
Raw data	This study	NCBI BioProject: PRJNA1021938
Oligonucleotides		
IS1_adapter.P5 (A*C*A*C*TCTTTCCCTACAC GACGCTCTTCCG*A*T*C*T)	Meyer and Kircher[64]	Sigma Aldrich
IS2_adapter.P7 (G*T*G*A*CTGGAGTTCAGAC GTGTGCTCTTCCG*A*T*C*T)	Meyer and Kircher[64]	Sigma Aldrich
IS3_adapter.P5+P7 (A*G*A*T*CGGAA*G*A*G*C)	Meyer and Kircher[64]	Sigma Aldrich
IS7_short_amp.P5 (ACACTCTT TCCCTACACGAC)	Meyer and Kircher[64]	Sigma Aldrich
IS8_short_amp.P7 (GTGACTGGAGTTCAGACGTGT)	Meyer and Kircher[64]	Sigma Aldrich
IS5_reamp.P5 (AATGATACGGCGACCACCGA)	Meyer and Kircher[64]	Sigma Aldrich
IS6_reamp.P7 (CAAGCAGAAGACGGCATACGA)	Meyer and Kircher[64]	Sigma Aldrich

(*Continued on next page*)

Continued		
REAGENT or RESOURCE	SOURCE	IDENTIFIER
Index_Primer_P5 (AATGATACGGCG ACCACCGAGATCTACAC-8nt_Index-ACACTCTTTCC CTACACGACGCTCTT)	Meyer and Kircher[64]	Sigma Aldrich
Index_Primer_P7 (CAAGCAGAAGAC GGCATACGAGAT-8nt_Index-GTGACTGGAGTTCAGACGTGT)	Meyer and Kircher[64]	Sigma Aldrich
Software and algorithms		
EAGER version 1.92.55	Peltzer et al.[65]	https://github.com/apeltzer/EAGER-GUI
FastQC version 0.11.5	Andrews[66]	https://github.com/s-andrews/FastQC/releases
AdapterRemoval version 2.2.1a	Schubert et al.[67]	https://github.com/MikkelSchubert/adapterremoval/releases
BWA v0.7.17	Li and Durbin[68]	https://github.com/lh3/bwa/releases
MarkDuplicate (Picard) v2.15.0	Broad Institute[69]	https://github.com/broadinstitute/picard/releases
DamageProfiler version 1.0	Neukamm et al.[70]	https://github.com/Integrative-Transcriptomics/DamageProfiler/releases
CircularMapper version 1.0	Peltzer et al.[65]	https://github.com/apeltzer/CircularMapper/releases
Bowtie2 v2.3.4.2	Langmead and Salzberg[71]	https://bowtie-bio.sourceforge.net/bowtie2/index.shtml
Trimmomatic v0.35	Bolger et al.[72]	http://www.usadellab.org/cms/?page=trimmomatic
VarScan v2.3.9	Koboldt et al.[73]	https://varscan.sourceforge.net
snpEff v4.3	Cingolani et al.[74]	https://pcingola.github.io/SnpEff/
SeqPrep	https://github.com/jstjohn/SeqPrep	https://github.com/jstjohn/SeqPrep
Integrative Genomics Viewer v2.4.8	Robinson et al.[56]	https://igv.org
Fastp v0.23.4	Chen et al.[75]	https://github.com/OpenGene/fastp/releases
FigTree v1.4.4	http://tree.bio.ed.ac.uk/software/figtree/	http://tree.bio.ed.ac.uk/software/figtree/
BRIG v0.95	Alikhan et al.[76]	https://sourceforge.net/projects/brig/
MEGA X v10.2.6	Kumar et al.[77]	https://www.megasoftware.net/

RESOURCE AVAILABILITY

Lead contact

Further information and requests for resources and reagents should be directed to and will be fulfilled by the lead contact, Verena J. Schuenemann (verena.schuenemann@iem.uzh.ch).

Materials availability

This study did not generate new unique reagents.

Data and code availability

- The raw sequencing data produced in this study will be available on publication under NCBI BioProject: PRJNA1021938.
- This study did not generate any unique code.
- Any additional information required to reanalyze the data reported in this paper is available from the lead contact upon request.

EXPERIMENTAL MODEL AND SUBJECT DETAILS

Ethics

All human samples were taken from anonymous remains more than 70 years old, and therefore do not require ethical approval for the genetic analysis under current Swiss law (https://www.admin.ch/opc/de/classified-compilation/20061313/index.html). As the remains are English, British law is also relevant: The remains studied here are more than 100 years old and as such they do not fall under the Human Tissue Act of 2004. Ethical approval was obtained from the Department of Archaeology, University of Cambridge (ARCH-09-2019-01) according to departmental guidelines for the PhD project of Alette A. Blom, for which samples presented in this study

were collected. Samples were provided under agreements of scientific collaboration. Directly involved people from the respective skeletal collections (Winchester Leprosarium curated at the University of Winchester, UK and Staple Gardens curated at Hampshire Cultural Trust) fully support this study and are co-authors. We also followed guidance for the ethical treatment of human remains following BABAO (https://www.babao.org.uk/assets/Uploads/BABAO-Code-of-Ethics-2019.pdf).

Human sample selection

Samples from human remains were selected in collaboration with the collection recorder (Dr. Katie White-Iribhogbe) and curator (Dr. Heidi Dawson-Hobbis). Individuals selected came from material that was excavated at a later stage and not yet published, or well-researched with biomolecular approaches. Relevant cases were chosen across a spectrum of leprosy-expression, including several without pathological lesions. The preference for sample elements, in order of preferred to less preferred, is as follows: loose fragments of internal nasal bones (these were never broken or cut off other bone (fragments)), maxillary frontal or lateral incisors or canines, calculus from any tooth, finger or foot bones with lesions, fibulae or tibiae fragments. For each individual a tooth was sampled if a loose nasal bone was not available, along with a bone (fragment) and both were sampled for intra-individual comparison. Where bones with pathologies were selected, the pathology was always avoided during the sampling process. Each tooth and bone (fragment) was photographed from all directions both before and after sampling. An exact list of samples taken can be found in Table S1. Skeletons 50, 60, 63, 64, 72, 80, 81, 87, 94, 101 and 117 were selected for sampling. Only the positive cases (skeleton 50, 80 and 94) will be discussed more elaborately below. Quantitative pathology scores and sample information are provided in Table S1.

Human remains: St Mary Magdalen, Winchester

The historically-known existence of the St Mary Magdalen leprosarium was confirmed by Time Team in 2000. Larger scale excavations in 2008-2015 – under the Magdalen Hill Archaeological Research Project (MHARP) – have unearthed 127 individuals, with the first 54 officially published (pers. comm. Katie White-Iribhogbe and Heidi Dawson-Hobbis). Of these 127 individuals, 43 show no diagnosable skeletal signs of leprosy, 33 cases show possible lesions, 20 cases show probable lesions and 22 cases show pathognomonic lesions. Nine individuals were too incomplete to diagnose leprosy. This paper qualitatively describes the leprosy-related lesions in the individuals who tested positive for *M. leprae*, and provides quantitative pathology scores for all sampled cases.

The first documentary reference to the hospital dates from 1148, with a later refoundation in 1180 likely by Richard of Ilchester, Bishop of Winchester.[78,79] The hospital's location adjacent to a major road was good for alms collection -, and next to open fields – which was good for renting.[42] Historic records refer to the hospital as a specific leper-care centre between 1325 and the late 15th century, then turning into a poor house.[79] They also indicate a history of rebuilding in and around the hospital, which is corroborated in the archaeological data. The earliest small stone-built structure was surrounded by wooden buildings, an early chapel and cemetery in the north, yielding 38 burials.[40,42] Overlaying these earliest structures is a stone phase from the mid-12th century, an extension of the hall and the addition of an infirmary, formal cloister and refurbishment of the chapel.[40–42] A new cemetery area also came into use south of the chapel, while the northern cemetery fell out of use. Only five burials were unearthed in this area, while 11 individuals were uncovered within the chapel.[40] In the subsequent two centuries, the hospital underwent several rebuilding episodes, as did the aisles of the chapel. The master's lodge was added to the infirmary's hall, and the new aisles contained a further nine graves.[40,42] The individuals sampled in this study all originate from the east side of the stone chapel, and likely date to the early 12th century.

Skeleton descriptions St Mary Magdalen Winchester

Skeleton 50 (MMW_H50) Skeleton 50 represents an individual that is 60-80% complete with a slightly fragmented skeleton and reasonable preservation. Age and sex estimation indicates they are a 26-45 year old male. Stature estimate: 175.412 cm +/− 3.27cm (femur: 47.9cm). This individual probably had leprosy based on a number of distinctive skeletal pathologies. The nasal spine area showed some taphonomic damage obstructing the observation of nasal spine absorption. There is slight resorption of the anterior maxillary alveolar bone surrounding the central incisors. The oral surface of the palate shows a slight increase of micro- and macroporosity that is not matched on the nasal surface of the palate. The nasal aperture is substantially enlarged in both latero-inferior portions. Nine proximal and 6 interproximal hand phalanges show slight concentric remodelling and one proximal hand phalanx shows some new periosteal bone formation. Both tibiae and fibulae show moderate new periosteal bone formation along the whole length, and the left cuboid, navicular, intermediate and lateral cuneiform show dorsal exostosis formation. The right MT1, MT3, MT4 and MT5 show concentric remodelling, new periosteal bone formation and distal absorption. The right MT2 is absent. The left MTs show no pathology. Four proximal foot phalanges show concentric remodelling and one proximal and one distal foot phalanx show distal resorption.

Skeleton 80 (MMW_H80) Skeleton 80 represents an individual that is 80-100% complete with a slightly fragmented skeleton with good preservation. Age and sex estimation suggest this individual is an 18-25 year old probable male. Stature estimate: 169.24 ± 2.99 (femur: 45.5cm; and tibia: 36.1cm). Pathological bone changes suggest this individual probably had leprosy. The anterior nasal spine shows a well-defined resorption and there is some resorption around the maxillary central incisors. The nasal surface of the palate shows a slight increase in microporosity, and the oral surface of the palate shows a substantial enlargement, deepening and increase of micro- and macroporosity though few true perforations to the nasal surface are identifiable. The nasal aperture shows an increase in porosity on the external surface accompanied by slight rounding of the latero-inferior portions of the opening. There is slight concentric remodelling of six interproximal hand phalanges, which also display volar grooving. The whole length of both tibiae

and both fibulae, and the right MT5 and left MT4 and MT5 have new woven periosteal bone formation and seven distal foot phalanges show distal notching.

Skeleton 94 (MMW_H94) Skeleton 94 represents an individual that is 80-100% complete with a slightly fragmented skeleton with good preservation. Age and sex estimation indicate that this individual is a 22-32-year-old male. Stature estimate: 169.105 ± 3.27 (femur: 45.25cm). Skeletal pathology indicates this individual possibly had leprosy. There is a well-defined reduction of the anterior nasal spine and some excess porosity around the nasal aperture. The oral surface of the palate shows a slight increase in the amount of microporosity. There are no changes in the lower arm or hands. The right tibia and fibula show some woven periosteal bone growth. The left tibia shows moderate new bone growth while the left fibula shows a severe amount of new periosteal bone growth that has caused thickening of the bone and changes to its normal cortical shape. The right MT1, MT2 and MT5 and the left MT2, MT4 and MT5 show some new periosteal bone deposits. Three proximal foot phalanges show concentric remodelling and 5 distal foot phalanges show notching of the distal ends.

Squirrel remains: Staple Gardens, Winchester

Development plans for a 4562m^2 plot at Northgate House in the western part of Staple House, Winchester triggered a series of archaeological interventions, building recording and excavations between 2002 and 2007. A total of 1821m^2 of Northgate House was archaeologically excavated.[80]

Staple House is located on Staple Gardens, a street first referred to in AD1110 as Bruhdenestret, and is closely associated with the Alfredian burh (burg, or fortified settlement) that was built in the 9th century along with a planned street grid and new defensive systems.[81] The excavations revealed a sequence of up to nine well-preserved properties, although most of the material dates to the 12th and 13th centuries. The front face of several of these properties faces east, with pits and post holes to the rear of the buildings, essentially forming a street front. The occupation and industrial activity along this street appear to decline by the late 12th-early 13th century, leading to a massive re-organisation of plot boundaries,[82] including a substantial plot to the west of Staple Gardens belonging to the archdeacon of Winchester.[82]

One property shows a substantial amount of craft waste, including evidence for furrier activity, high status food preparation and smithing: property SE1. Although there is evidence of habitation on this property from AD825 onwards, the majority of building remnants date to the 11th-13th century.

On the east side of SE1, a pit (NH5169) dating to the 12th-13th centuries was found,[37] measuring 1.35m in diameter and 1.45m deep. The pit contained a rich assemblage of kitchen waste and ash, likely from domestic ovens and hearths.[36] Among the kitchen waste a myriad of fish bones were found, belonging predominantly to herring, but also bones from garfish, cod, whiting, ling, flounder, plaice, mackerel and a sturgeon bone. Sturgeon is generally considered to be a high status food source, and this, along with the finding of many burnt bones - indicative of roasting - point towards the deposit of higher status food remains.[36] More interestingly, however, the pit contained a total of 745 unburnt bones of cat, fox, squirrel, ferret/polecat, stoat, and other unidentified small mammals. Except for the cat remains, the bones consisted exclusively of foot and leg bones, characteristic of fur production and trade. The skinning itself likely occurred at another location, with the pelts being transported with the foot and leg bones attached, only to be removed at the final destination.[37] Although impossible to say based on the current archaeological data, these pelts may have been traded in from Russia, Scandinavia or elsewhere in Britain,[83] depending on the style, quality and colour desired by the local wealthy. The cat remains represent most skeletal elements and consisted of at least 10 individuals aged between 8.5 and 11.5 months and show some signs of cut marks, indicating that the skinning of cats did happen on site.[37] The same pit also contained bones belonging to neonatal lambs possibly related to small garment or parchment production, although evidence for the latter is scarce.[37,83]

Five metres to the northeast, also along the property boundary, a cesspit (NH5175) measuring 1.2 by 0.9m across and 0.64meter deep was uncovered, dating to the same period as pit NH5169. This pit contained several fruit pits in the bottom, including a grape pip - again a high-status food source and likely imported. The upper fill of this pit also contained several cat bones and one fox bone, suggesting further furrier activity. This pit also contained a variety of fish remains, including sea bream and scad.[36] Several metres to the northwest of pit NH5169, another pit (NH5198) also revealed some signs of furrier activity, including some ferret remains and the foot of another small mammal with several cut marks. To the southeast of the property boundaries, a pit (NH5105) revealed an equal-armed balance, used for weighing valuable items, and revealed a smithing hearth bottom.[36]

Fox and squirrel were often used by members of the lesser nobility and merchants, whilst cat fur and coarse lambskin (budge) were the cheapest furs available to purchase. Thus, overall the pits to the rear of property SE1 show a variety of crafts being performed, focussing on the production or sale of items and food for the wealthier and higher-status citizens of Winchester. Around the time that property SE1 was in use, Winchester had become the capital of Wessex, and a bishopric, and high quality fur was probably a popular commodity,[83] going hand-in-hand with an increased demand for other high-quality products. Simultaneously, however, lower quality fur remained popular among other classes of society and appear to have been produced on the same site.

Based on stratigraphic relationships to other elements of the site which have been dated through archaeomagnetic and radiocarbon dating, and historically referenced material culture sources (i.e., coins) the pit is interpreted as Phase 5, which starts at 1050AD and ends at 1225AD.[51]

Squirrel sample descriptions

Squirrel 1 (SGW_S1). Left calcaneus. Possible new periosteal bone formation showing as 'rough' bone surface in sustentacular sulcus. Could also be taphonomic alteration.

Squirrel 2 (SGW_S2). Right tibia (distal half). No pathology.

Squirrel 3 (SGW_S3). Right fourth metatarsal. Possible new periosteal bone formation, showing as 'rough' bone surface of distal head. Could be taphonomic alteration.

Squirrel 4.1 (SGW_S4.1). Right fifth metatarsal. Potential slight new periosteal bone formation at the proximal end of the metatarsal.

Squirrel 4.2 (SGW_S4.2). Left third metatarsal. Possible new periosteal bone formation, showing as 'rough' bone surface of distal head. Could be taphonomic alteration.

Squirrel 6 (SGW_S6). Foot or hand proximal phalanx. Small, smooth bone nodule towards the proximal end of the phalanx.

Squirrel 7 (SGW_S7). Left first metacarpal. No pathology.

Squirrel 8 (SGW_S8). Foot or hand proximal phalanx. Phalanx shows substantial, active periosteal bone formation along the medial and lateral sides of the diaphysis.

Squirrel 9 (SGW_S9). Left first metacarpal. No pathology.

Squirrel 10 (SGW_S10). Foot or hand proximal phalanx. Substantial, though well-healed, periosteal bone growth along the diaphysis; most pronounced on the medial and lateral side of the distal half of the diaphysis. Medial-lateral border is almost doubled in width.

Squirrel 11 (SGW_S11). Foot or hand proximal phalanx. Distal head is altered in shape due to well-healed, lumpy bone growth and two bony extensions just proximal to the head. Both the head and the nodules have several macropores and sharp-crested bony ridges.

METHOD DETAILS

Human osteology and palaeopathology

All human remains were analysed by Katie White-Iribhogbe between 2011 and 2016,[43] and re-analysed by Alette A. Blom in 2022 based on the new BABAO guidelines.[84] Leprosy pathologies were recorded both qualitatively and quantitatively. The written descriptions (qualitative) are summarised above.

Assessment of leprosy-related lesions was based on work by Møller-Christensen primarily[85] along with more recent work,[86–98] adapted by Alette A. Blom. Each site that can be involved in what is often dubbed 'rhinomaxillary syndrome' is scored independently on a four to six scale system to both ease intra-site comparison and acknowledge that not all sites may be simultaneously involved. Images of the different scores for each feature can be found in Figure S1 Leprosy Scores. The anterior nasal spine (ANS) can show absorption of the spine and eventual rounding of the inferomedial portion of the nasal aperture; this process is scored in 4 stages. The alveolar process of the maxillary incisors (APM) can show superior and lateral absorption of the tooth sockets and potential eventual loss of the maxillary incisors, which is scored in 4 stages. The nasal surface of the palate (PPMN) can show increased micro- and macroporosity, sharp and/or porous new bone formation, and eventual perforation through the PPMN, which is scored in 4 stages. Changes to the oral surface of the palate (PPMO) can also show increased micro- and macroporosity, sharp and/or porous new bone formation and eventual perforation through initially the PPMO and then PPMN, which is scored in 6 stages. Finally, the rounding and/or enlargement/reduction of the nasal piriform opening (NPI) in infero-lateral direction is scored in 6 stages. New periosteal bone formation on the radii and ulnae, and fibulae and tibiae are scored on a 4 stage system: 1) no new periosteal bone formation (NPBF), 2) slight NPBF, 3) moderate NPBF; and 4) severe new NPBF. For all tarsals, metacarpals and metatarsals, and phalanges it is recorded whether they have a number of characteristic changes described in previous literature (including dorsal exostosis, knife-edge remodelling, NPBF, abscess formation, distal absorption, stumping, concentric remodelling, volar grooving, notching of the dismarginal tufts, phalangeal buttoning, pen-in-cup articulations and granulomatous lesions). For overview of these scores per samples skeleton, see Table S1.

Sampling and DNA extraction

Strict guidelines for ancient DNA processing were followed for all pre-PCR parts of the workflow.[99] Sampling was performed in a dedicated ancient DNA cleanroom facility at the University of Zurich. All samples were UV irradiated from all sides for 30 min each to minimise modern DNA contamination on the surface. For human bone samples, a part of the bone surface was removed by using a dental drill prior to sampling to further reduce the risk of introducing modern DNA contamination, followed by sampling with a fresh dental drill bit. Human tooth samples were sampled using a dental drill from inside the pulp for the same reason. Due to the small amounts of squirrel bone and human calculus, these samples were directly powdered after UV treatment using a mortar and pestle.

DNA extraction of approximately 50 mg powdered sample is based on a well-established silica-based protocol.[100] See Table S1 for exact amounts of extracted material per sample. Negative controls were included and carried along until sequencing and analysis to trace any potential contamination. Per sample (< 100 mg sample powder) 1000 μL or 1500 μL (> 100 mg sample powder) of extraction buffer (0.45 M EDTA pH 8.0, 0.25 mg/mL Proteinase K) were used and incubated 18 h overnight at 37°C on a shaker. On the next day, insoluble remains were pelleted for 5 min at maximum speed in a benchtop centrifuge. The supernatant was mixed with 10x volume of binding buffer (5 M guanidine hydrochloride, 40% isopropanol), applied to a Qiagen MinElute column, and centrifuged at maximum speed for 1 min. The column was washed twice by 600 μL PE Buffer followed by dry spinning at maximum speed. 50 μL of Tris-EDTA-Tween (TET) Buffer (1 mM EDTA pH 8.0, 10 mM Tris–HCl pH 8.0, 0.05% Tween 20) was added to the column and incubated for 5 min. Eluate was collected in a 1.5 mL Eppendorf tube. Elution was repeated once and both eluates were combined for a total of 100 μL.

Double-stranded library construction and double indexing

Strict guidelines for ancient DNA processing were followed for all pre-PCR parts of the workflow.[99] Library preparation was performed in four steps based on a well-established protocol.[64,101] In short, the following steps were carried out. First, blunt-end repair was performed by combining 20 μL of DNA extract with 30 μL of Blunt End Repair Master Mix in a 0.2mL PCR tube for final reaction concentrations of 1x NEBuffer 2.1, 0.1 mM dNTP mix, 0.8 mg/mL BSA, 1mM ATP, 0.4 U/μL T4 Polynucleotide kinase, 0.024 U/μL T4 Polymerase. The reaction was incubated for 15 min at 15°C followed by 15 min at 25°C in a PCR cycler. The reaction cleanup was performed with Qiagen MinElute columns according to the manufacturer's instructions. Blunt-ended fragments were eluted in 18 μL of TET buffer in 1.5 mL Eppendorf tube.

Library adapters were ligated by adding Adapter Ligation Master Mix to the 18 μL of blunt-ended eluate in the 1.5 mL for a final reaction concentration of 1x Quick Ligase Buffer, 250 nM Solexa Adapter Mix, and 0.125 U/μL Quick ligase. After mixing, the adapter ligation reaction was incubated for 30 min at room temperature followed by a Qiagen MinElute cleanup and elution in 20 μL of TET.

The eluate was transferred to a new 0.2 mL PCR tube and adapter fill-in was performed by adding Adapter Fill-In Master Mix for a final reaction volume of 1x Isothermal buffer, 125 μM dNTP mix, 0.4 U/μL Bst polymerase 2.0 followed by incubation for 20 min at 37°C and 20 min at 80°C in a PCR cycler. No cleanup was performed.

For the indexing reaction, the heat-inactivated adapter fill-in reaction was directly split in 4 0.2 mL PCR tubes (10 μL each) and 2 μL P5 index primer (10 μM) and 2 μL P7 index primer (10 μM) were added. The reactions were each topped up to 100 μL with Indexing Master Mix for final reaction concentrations of 1x Pfu Turbo Buffer, 25 μM dNPT mix, 0.15 mg/mL BSA, 0.025 U/μL Pfu Turbo Cx HotStart Polymerase. The reactions were transported to the post-PCR lab and run in a thermocycler using the following profile: 2 min at 98°C, followed by 10 cycles of 30 s at 98°C, 30 s at 58°C and 60 s at 72°C. A final incubation of 10 min at 72°C concluded the PCR profile. Reaction cleanup was performed with MinElute columns according to the manufacturer's instructions and eluted in 50 μL TET.

If necessary, the double-indexed libraries were further amplified aiming for a final concentration of 200 ng/μL. For this, four 100 μL reactions per library (5 μL DNA library input) were set up with the final reaction concentrations of 1x Herculase II Reaction Buffer, 0.25 mM dNTP mix, 0.4 μM IS5 Primer,[64] 0.4 μL IS6 Primer[64] and 1.0% (v/v) Herculase II Fusion DNA Polymerase. The reactions were run a PCR cycler using the following profile: 2 min at 95°C, followed by 2 - 12 cycles (depending on input DNA concentration) of 30 s at 95°C, 30 s at 60°C and 30 s at 72°C. A final incubation of 5 min at 72°C concluded the PCR profile. All four reactions of a single library were pooled and Qiagen MinElute cleanup was performed according to the manufacturer's instructions. Quality control was performed for the amplified libraries on the Agilent TapeStation using D1000 tapes.

Shotgun sequencing

Sequencing was performed by the Functional Genomics Center Zurich and the Vienna BioCenter Next Generation Sequencing Facility. Paired-end sequencing was performed using 2*75 + 8+8 cycles on a NextSeq500 platform using standard Illumina protocols.

Initial *M. leprae* myBait full genome enrichment

Libraries of all potentially positive samples and corresponding negative controls were enriched for *M. leprae* genomic fragments using myBaits v4 in-solution hybridization capture (Arbor Biosciences, design: 180220-90; based on *M. leprae* Br4923[102]). One round of capture was applied following the manufacturer's instruction for enriching low copy, degraded or contaminated DNA libraries. In short, up to 2 μg of amplified library were used in input for the enrichment reaction. The enrichment was carried out at 65°C for 48 h. The enriched libraries were PCR amplified and were used for sequencing as described before.

Additional library preparation for SGW_3_1

All of the remaining aDNA extract for *M. leprae* positive squirrel sample SGW_3_1 was used in a second library preparation round and shotgun sequenced as described before.

Second *M. leprae* myBait full genome enrichment

Both libraries for SGW_3_1 were enriched for *M. leprae* genomic fragments using myBaits v4 in-solution hybridization capture (Arbor Biosciences, design: 180220-90; based on *M. leprae* Br4923[102]). Two rounds of capture were applied following the manufacturer's manual instruction for enriching low copy, degraded or contaminated DNA libraries. In short, 2 μg of amplified library were used in input for the enrichment reaction. The enrichment was carried out at 65°C for 48 h. The enriched libraries were PCR amplified and 2 μg were used as an input for a second round of enrichment. Libraries from both rounds of enrichment were used for separate rounds of sequencing.

HyperExplore bait capture of SGW_3_1 and data analysis

A second *M. leprae* enrichment was applied to overcome a possible enrichment bias of the myBaits method and to potentially increase the overall coverage for the squirrel sample. Two libraries (prepared at University of Zurich) were target enriched for the *M. leprae* genome using the KAPA HyperExplore Max 3Mb custom bait capture kit (Roche, IRN 1000013073, *M. leprae* Br4923) at Colorado State University. Around 1 μg of each library was used in single capture according to the KAPA HyperCap Workflow (v3.2). Each enrichment was followed by an amplification step using the Kapa library amplification kit following manufacturer recommendations and a purification step using AMPure beads. Libraries were quantified using the Qubit dsDNA BR (Thermofisher) kit and

the quality was assessed on a TapeStation 4150 using the D1000 screen tape (Agilent). Libraries were pooled and sequenced single end on a NextSeq 500 instrument.

The sequencing quality has been assessed with FastQC version 0.11.5[66] before reads were adapter-trimmed and paired-end reads were merged (AdapterRemoval version 2.2.1a[67]). All pre-processed reads from SGW_3_1 were combined for further analysis. Preprocessed reads were then mapped onto the *M. leprae* TN reference genome (GenBank AL450380.1) with Bowtie2 v2.3.4.2.[71] Putative unique variants of the strain were manually checked and visualised using the Integrative Genomics Viewer.[56]

Collagen extraction (St Mary Magdalen, human samples)

Collagen extraction for human samples was performed at the Dorothy Garrod Laboratory, University of Cambridge. The samples that were submitted for radiocarbon dating were collagen surplus for carbon and nitrogen isotope research for another project. All samples come from the single root of a second molar, cut off from the cemento-enamel junction using a diamond cutting wheel fit into a drill. Samples are subsequently sandblasted to remove any external contamination and prepared following a modified Longin method,[103,104] which will be described briefly. All samples were demineralised in 8 mL of cold 0.5 M HCl and kept refrigerated. The acid was changed every 2 days. When the samples were ready, the acid was decanted off and the samples thrice rinsed with distilled water. Samples were then submerged into 8 mL pH 3.0 water and heated at 75°C for 48 h with a plastic lid preventing evaporation. After full gelatinisation was achieved, the supernatant was filtered off using an Ezee filter. The samples were then frozen in a −20°C freezer overnight, and then moved to a −80°C freezer for 4 h before being placed in the freeze-drier for approximately 2 days. Three aliquots of collagen were weighed for stable isotope analysis and the surplus used for radiocarbon dating.

Collagen extraction (furrier pit, animal sample)

Since the whole SGW_3_1 sample was used up for DNA extraction, we used a cat bone from the same furrier pit for collagen extraction. Furrier's waste pits are probably in use for no more than a couple of years, suggesting that the two bones were deposited within a relatively short time of each other and the cat bone can be used as representative of the wider use-range of the pit. Collagen was extracted by the Laboratory of Ion Beam Physics at ETH Zurich (Laboratory number: ETH-127328) and purified using a modified ultrafiltration method from Hajdas and colleagues.[105] The collagen was then used for radiocarbon dating in the same laboratory.

Radiocarbon dating

Radiocarbon dating was performed by the Laboratory of Ion Beam Physics at ETH Zurich (Laboratory numbers: ETH-127328, ETH-138163, ETH-138164, and ETH-138165). Data calibration was done with OxCal v4.4.4.[106,107]

QUANTIFICATION AND STATISTICAL ANALYSIS

DNA preservation assessment for all Winchester samples

Reads from each human sample were mapped to the complete human reference genome (GRCh38.p14). In short, all shotgun data for the same individual were merged together and were processed using EAGER version 1.92.55.[65] The sequencing quality has been assessed with FastQC version 0.11.5[66] before reads were adapter-trimmed and merged (AdapterRemoval version 2.2.1a[67]). Reads were mapped to a complete human reference (GRCh38.p14) using BWA[68] with a maximum edit distance of 0.01 and mapping quality 37. Duplicate reads were removed using MarkDuplicate[69] and aDNA damage assessed using DamageProfiler version 1.0.[70] Squirrel samples were analysed the same way, but mapped against *S. vulgaris* complete genome (GenBank: GCA_902686455.2).

Shotgun data screening for potential *M. leprae* positive human and squirrel samples

Shotgun sequencing data from the same sample was merged and pre-processed with EAGER as mentioned before. CircularMapper version 1.0[65] with a maximum edit distance of 0.01 and mapping quality 37 was used to align all reads to the complete *M. leprae* TN reference (GenBank: NC_002677.1). CircularMapper uses the BWA algorithm.[68] Duplicate reads were removed using MarkDuplicate[69] and aDNA damage assessed using DamageProfiler version 1.0.[70] The same was performed for an alignment to the *M. leprae* specific repetitive element RLEP (GenBank: AL450380.1 position 74457-75125), but with the BWA algorithm.

Squirrel sample species verification

We verified the Eurasian red squirrel origin of the animal bones used in this study from the bone pit. Reads from each animal sample were mapped against mitochondrial references for all the described species found in the fur pit (*Felis catus*, GenBank: NC_001700.1; *Mustela erminea*, GenBank: NC_025516.1; *Mustela putorius voucher*, GenBank: NC_020638.1; *Sciurus vulgaris*, GenBank: LR822068.1; *Vulpes vulpes*, GenBank: NC_008434.1). In addition, we mapped against mitochondrial references of human, mouse and rat (*Mus musculus*, GenBank: NC_005089.1; *Rattus rattus*, GenBank: NC_012374.1; *Homo sapiens*, GenBank: NC_012920.1). In short, all shotgun data from the same sample was merged together. We used EAGER version 1.92.55[65] to process all reads. The sequencing quality has been assessed with FastQC version 0.11.5[66] before reads were adapter-trimmed and merged (AdapterRemoval version 2.2.1a[67]). Reads were mapped against the mitochondrial references using CircularMapper version 1.0[65] with a maximum edit distance of 0.01 and mapping quality 37. Duplicate reads were removed using MarkDuplicate[69] and aDNA damage assessed using DamageProfiler version 1.0.[70]

Data analysis of *M. leprae* enrichment (BWA)

Sequencing data from the same sample was merged and pre-processed with EAGER as mentioned for shotgun data. CircularMapper version 1.0[65] with a maximum edit distance of 0.2 and mapping quality 37 was used to align all reads to the complete *M. leprae* TN reference (GenBank: NC_002677.1). CircularMapper uses the BWA algorithm.[68] Duplicate reads were removed using MarkDuplicate[69] and aDNA damage assessed using DamageProfiler version 1.0.[70] The same parameters were used for an alignment to the *M. leprae* specific repetitive element RLEP (GenBank: AL450380.1 position 74457-75125), but with the BWA algorithm.

Data analysis of *M. leprae* enrichment for human samples (Bowtie2)

Raw reads were processed as described elsewhere.[108] Briefly, reads were adapter- and quality-trimmed with Trimmomatic v0.35[72] for quality score greater than 15 and length greater than 40 with a 5-base wide sliding window using Trimmomatic version 0.35.[72] Illumina adapters were removed using the Trimmomatic option Illuminaclip allowing maximally 2 mismatches and a minimum score of 30 for pair-end reads. Reads were merged using SeqPrep (https://github.com/jstjohn/SeqPrep) and mapped onto the *M. leprae* TN reference genome (GenBank AL450380.1) with Bowtie2 v2.3.4.2.[71] SNP calling was done using VarScan v2.3.9.[73] To avoid false-positive SNP calls, duplicate reads were omitted from downstream analyses and the following cutoffs were applied for VarScan: minimum overall coverage of five non-duplicated reads, minimum of three non-duplicated reads supporting the SNP, mapping quality score >8, base quality score >15, and a SNP frequency above 80%. All Variant Call Format (VCF) files were analysed using snpEff v4.3.[74] Heterozygous sites (20-80% SNP frequency), repetitive regions and ribosomal RNA genes in the reference sequence were omitted.

SGW_3_1 read truncation for phylogenetic analysis

To remove the characteristic aDNA deamination pattern, which accumulates at the ends aDNA fragments,[52] paired end reads were merged as described before and then trimmed by 1 nt, 2 nt, 3 nt, or 4 nt on both sides using fastp without any additional filtering.[75] Reads then underwent further pre-processing and mapping as described in the BWA and Bowtie2 data analysis sections.

Genotyping of SGW_3_1 using partial genome sequencing

Because of the low coverage of SGW_3_1, SNP typing and phylogenetic position were done in two steps. To decipher the SNP typing of SGW_3_1, informative positions described by Monot and colleagues[55] (82 positions) were checked manually using the Integrative Genomics Viewer.[56] SNP and coverage for each of these positions are presented in Table S4. Manual genotyping revealed that SGW_3_1 belongs to the genotype 3I (Branch 3). To decipher the phylogenetic position of SGW_3_1 in the Branch 3, informative SNPs specific to genomes from the branch 3 and the clusters of strains inside the branch 3 were obtained from the comparative genomics of 49 strains, based on Bowtie 2 mappings, including strains from the genotype 3I (n = 48), the genotype 3L (Abusir1630[4]) as outgroup and two references (TN and Br4923) (Figure S2). The analysis resulted in 299 informative positions (Table S5) that were checked manually (SNP and coverage) in SGW_3_1 using the Integrative Genomics Viewer.[56] This approach allowed us to pinpoint the branching of SGW_3_1 in the tree. However, deeper coverage would be needed to evaluate the exact length of the branch as this approach does not analyse specific SNPs of SGW_3_1.

Phylogenetic tree construction

Phylogenetic placement of the newly reconstructed strains was performed based on at least 80% covered positions in the SNP alignments. The Maximum Likelihood tree was constructed with extensive Subtree-Pruning-Regraftig in MEGA X[77] and 1000 bootstraps starting from an automatically generated initial Maximum Parsimony tree.

For the tree with only the three new human samples General Time Reversible model[109] tested as the best model, whereas Kimura 2-parameter model[110] was used for the reduced phylogeny with the squirrel sample.

FigTree v1.4.4 (http://tree.bio.ed.ac.uk/software/figtree/) was used to visualise all trees.

Coverage plots

Coverage plots were generated based on the duplicate read free alignments using BRIG.[76] Maximum value for each graph was set to three times the average coverage of the corresponding sample.